ChemComm

A Ruthenium Porphyrin-Based Porous Organic Polymer for the Hydrosilylative Reduction of CO2 to Formate

Journal:	*ChemComm*
Manuscript ID	CC-COM-03-2019-002273.R1
Article Type:	Communication

Journal Name

COMMUNICATION

A Ruthenium Porphyrin-Based Porous Organic Polymer for the Hydrosilylative Reduction of CO_2 to Formate

Received 00th January 20xx,
Accepted 00th January 20xx

DOI: 10.1039/x0xx00000x

www.rsc.org/

Grace. M. Eder, David. A. Pyles, Eric Wolfson, and Psaras. L. McGrier*

A ruthenium porphyrin-based porous organic polymer (POP) was synthesized, characterized, and used to reduce CO_2 to a formate salt. We demonstrate that Ru-BBT-POP can be utilized to reduce CO_2 to a silyl formate and then converted to potassium formate with a respectable turnover number and frequency.

The continuous accumulation of carbon dioxide (CO_2) in the atmosphere is believed to be one of the biggest contributors to rising sea levels and climate change.[1] As a consequence, CO_2 capture and conversion has become a desirable way to not only convert this abundant C_1 building block into a useful feedstock for high-value commodity chemicals and fuels, but also to reduce the worlds dependence on fossil fuels.[2] For example, the catalytic hydrogenation of CO_2 to methanol or formic acid has the potential to create alternative energy sources.[3] In particular, formic acid is of considerable interest because it is a liquid at ambient temperature and has a high volumetric hydrogen density of 53 g L^{-1} making it a viable hydrogen storage material.[4] In addition, formic acid also exhibits low-toxicity, which makes it more environmentally safe than petrochemicals. Although the hydrogenation of CO_2 to formic acid has been achieved using a variety of homogeneous catalysts composed of noble transition metals,[5-7] difficulties associated with recyclability and catalyst separation are still common for most systems. This leaves plenty of room to design heterogeneous catalytic systems for CO_2 capture and conversion that are stable, recyclable, and exhibit high efficiencies.

Porous organic polymers (POPs)[8,9] have emerged as an exceptional class of amorphous porous materials suitable for heterogeneous catalytic applications due to their superior chemical stability, high surface areas, and tunable pore sizes. These characteristics enable the prompt diffusion of substrates and products throughout the catalytic process. The modular nature of POPs permits the integration of various metalated organic linkers to efficiently convert CO_2 into a value-added chemical or fuel. For instance, one common strategy often employed is the reaction of epoxides with CO_2 to form cyclic carbonates in the presence of metalated porphyrin- and bypyridine-based POPs.[10-13] Recently, Yoon and coworkers demonstrated that an amorphous covalent triazine framework (CTF) decorated with Ir(III)-N-heterocyclic carbene complexes is very effective at converting CO_2 into a stable formate salt in the presence of an amine solution and H_2.[14] Liu and coworkers have also shown that an amorphous microporous organic polymer (MOP) containing Troger's base and a Ru(III) complex is also effective at performing this transformation under similar reaction conditions.[15] In contrast to these methods, the reduction of CO_2 using hydrosilanes has also emerged as an alternative route to functionalize CO_2 by trapping it as a silyl formate. In addition to being a favorable thermodynamic process, silyl formates are advantageous because they can be converted directly to formic acid/formate or an array of carbonyl compounds simply by reacting them with the proper nucleophiles.[16] Although many homogeneous catalytic systems using transition metals (Ru,[17] Ir,[18] Ni,[19] Zr,[20] Cu,[21] and Zn[22]) have been reported for the hydrosilylation of CO_2, examples of performing this transformation under heterogeneous catalytic conditions has yet to be reported.

Herein, we present the synthesis, characterization, and catalytic properties of a benzobisthiazole (BBT)-linked Ru(II) porphyrin-based POP (Ru-BBT-POP) (Scheme 1). We demonstrate that Ru-BBT-POP is an effective catalyst for the reduction of CO_2 to silyl formate using hydrosilanes. The silyl formate was then efficiently converted to potassium formate with a respectable turnover number and frequency.

Ru-BBT-POP was synthesized by reacting premetalated Ru(II)-tetrakis(4-formylphenyl)porphyrin (Ru-TFPP) with 2,5-diamino-1,4-benzenedithiol dihydrochloride (DABTD) in a 1:1 (v/v) mixture of DMF and *o*-xylenes at -78 °C for 5 h to avoid prompt precipitation of the imine-linked intermediate. Afterwards, the reaction mixture was gradually brought to room temperature overnight, and

[a] *Department of Chemistry & Biochemistry, The Ohio State University, Columbus, Ohio 43210, United States*

† Electronic supplementary information (ESI) available: Synthetic procedures, FT-IR, solid-state ^{13}C NMR, TGA, PXRD, and SEM. See DOI: 10.1039/x0xx00000x

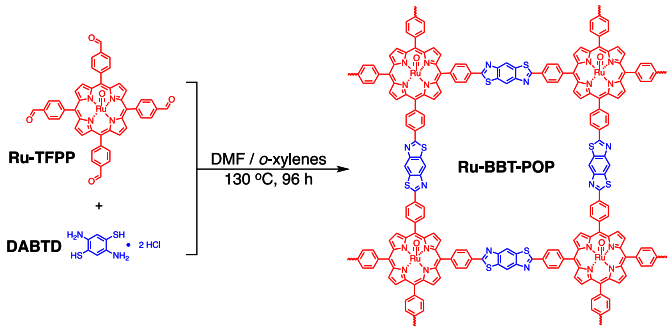

Scheme 1 Synthesis of Ru-BBT-POP 1.

then stirred under air at 130 °C for 96 h. Ru-BBT-POP was obtained by filtration and washed with acetone to produce dark red solids. Ru-BBT-POP was purified by soaking the polymer in methanol and dichloromethane for two days to remove unreacted monomers and then dried under vacuum. Powder X-ray diffraction (PXRD) analysis revealed that Ru-BBT-POP was amorphous and exhibited no long-range order (Fig. S5, ESI).

Ru-BBT-POP was characterized by Fourier transform (FT-IR) and ^{13}C cross-polarization magic angle spinning (CP-MAS) spectroscopies. The FT-IR spectra revealed stretching modes at 1654 (C=N) and 713 cm^{-1} (C-S), which is indicative of the formation of the benzothiazole ring (Fig. S3, ESI). The strong resonance at 1938 cm^{-1} is attributed to the carbonyl ligand bound to Ru(II) center. The FT-IR peaks corresponding to the phenyl and pyrrole substituents were also confirmed (Fig. S3 and Table S3, ESI). The connectivity of Ru-BBT-POP was verified by ^{13}C CP-MAS exhibiting a resonance at 167.0 ppm that corresponds to the central carbon on the benzothiazole ring, and resonances at 124.2 and 119.9 ppm, which correspond to the pyrrole substituents (Fig. S6, ESI). Diffuse reflectance UV-vis spectroscopy was also used to verify the presence of the porphyrin units of Ru-BBT-POP (Fig. S20, ESI). Thermogravimetric analysis (TGA) indicated that Ru-BBT-POP retained ~ 90 % of its weight up to 380 °C (Fig. S7, ESI). Scanning

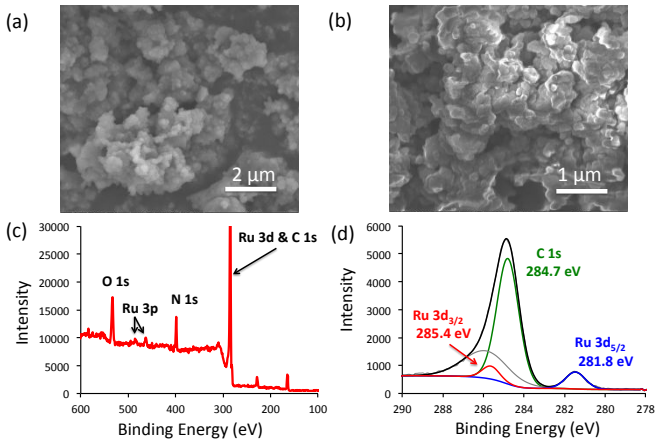

Fig. 1 SEM images at different magnifications (a and b) and XPS spectra (c and d) of Ru-BBT-POP.

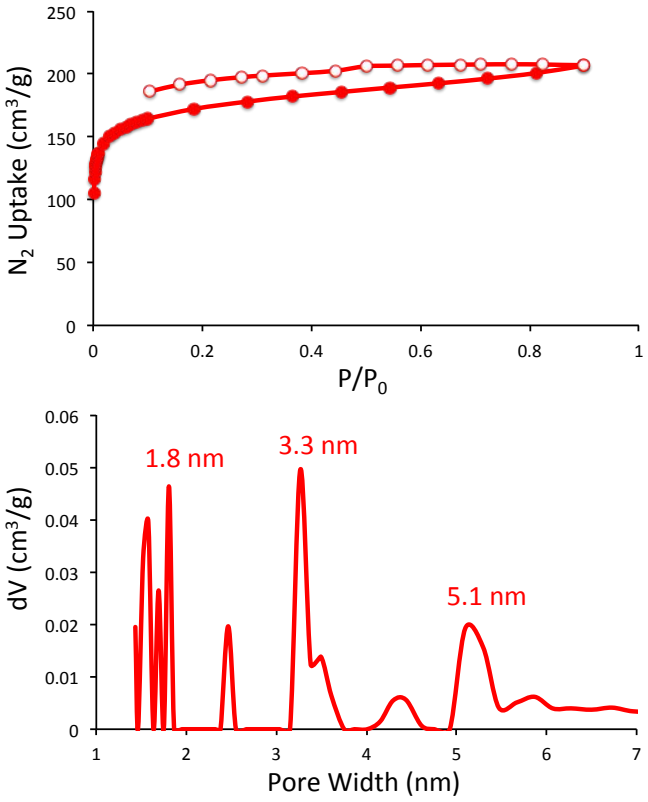

Fig 2. Nitrogen adsorption/desorption isotherm (top) and NLDFT pore size distribution (bottom) for Ru-BBT-POP.

electron microscopy (SEM) images revealed a cloud-like morphology for the material (Figures 1a and b).

X-ray photoelectron spectroscopy (XPS) of Ru-BBT-POP further confirmed the presence of Ru on the polymer surface (Fig. 1c and d). The broad signals at 281.8 and 285.4 eV correspond to the core energy levels of Ru $3d_{5/2}$ and Ru $3d_{3/2}$, respectively. The broad peak at 281.8 eV is typical for Ru(II) species bound to nitrogen-based ligands, and further confirms that Ru(II)-porphyrin complexes are embedded within the POP.[23,24] The presence of the carbon, nitrogen, and oxygen atoms of Ru-BBT-POP were also confirmed by XPS. Inductively coupled plasma-atomic emission spectroscopy (ICP-AES) analysis indicated that ~ 6.32 wt% (0.75 mol%) of Ru was incorporated into Ru-BBT-POP.

The permanent porosity of Ru-BBT-POP was measured by nitrogen gas adsorption at 77 K (Fig. 2). Ru-BBT-POP exhibited a reversible type I isotherm with a noticeable hysteresis. Application of the Brunauer-Emmett-Teller (BET) model over the low-pressure region ($0.001 < P/P_0 < 0.069$) provided a surface area of 655 m^2/g. Nonlocal density functional theory (NLDFT) was used to estimate the pore size distribution of the material yielding values of 1.8, 3.3, and 5.1 nm. This broad pore size distribution is not uncommon for amorphous porous polymers and is attributed to interparticle voids that can mimic sizeable pores. The total pore volume was calculated

Table 1 Catalytic Performance of Ru-POR and Ru-BBT-POP for the reduction of CO_2 to formate.

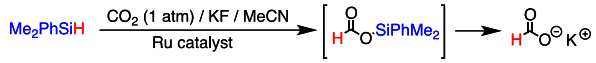

Entry	Ru catalyst (mol %)	Additive	% Yield[e]	TON[f]	TOF (h^{-1})[g]
1[a]	Ru-POR (0.5)	Me_2PhSiH	55	110	28
2[b]	Ru-POR (0.5)	Me_2PhSiH	0	0	0
3[c]	Ru-BBT-POP (0.5)	Me_2PhSiH	25	66	17
4[d]	Ru-BBT-POP (1)	Me_2PhSiH	41	54	14

[a]Reaction conditions: 4 mg (0.005 mmol) of Ru-POR was added to 10 mL of MeCN containing Me_2PhSiH (1 mmol), KF (1 mmol), and 1 atm of CO_2 at 60 °C for 4 h. [b]Performed without KF. [c]6 mg (0.005 mmol) Ru-BBT-POP. [d]9 mg (0.01 mmol) Ru-BBT-POP. [e]The yield of $HCOO^-K^+$ was determined by ^1H NMR (D_2O, 400 MHz) using DMSO as an internal standard. [f] Turnover number (TON) = mmol of formate/mmol of Ru. [g]Turnover Frequency (TOF) = TON per hour.

from the single point value of P/P_0 = 0.901 to provide a value of 0.312 cm^3 g^{-1} for Ru-BBT-POP. To assess the CO_2 uptake capacity of Ru-BBT-POP, we measured gas adsorption isotherms at 273 and 298 K from 0 to 1.2 bar (Fig. S13, ESI). Ru-BBT-POP displayed uptake capacities of 105 mg g^{-1} and 71 mg g^{-1} at 273 and 298 K. Isoteric heat of adsorption (Q_{st}) data revealed a high value of 48 kJ mol^{-1} at zero coverage, which is just below the lower limit for chemisorption (~ 50 kJ/mol). This indicates that the BBT-linkage and presence of Ru(II) significantly enhances the binding affinity for CO_2 due to a combination of Lewis acid/base[25] and metal ion•••quadrupole[26] interactions, respectively (Fig. S14, ESI).

In order to find the best reactions conditions suitable for the reduction of CO_2 to formate using inexpensive hydrosilanes and KF, we first examined the reactivity of CO_2 in the presence of various hydrosilanes at temperatures ranging from 45-80 °C (Table S6 & S7, ESI) using Ru-POR as a homogenous catalyst (Scheme S4, ESI). We found that the reactions that were carried out using Me_2PhSiH in MeCN at 60°C and 0.5 mol % Ru-POR for 4h at an initial CO_2 pressure of 1 atm provided the best results yielding a TON of 110 and a TOF of 28 h^{-1} (Entry 1 Table 1). While Me_2PhSiH provided the best results, increasing the temperature to 80 °C did not improve the efficiency of the reaction and resulted in a decrease in yields (Entry 3 Table S7, ESI). It is worth noting that reaction conditions in which KF was not used resulted in no formation of potassium formate (Entry 2 Table 1).

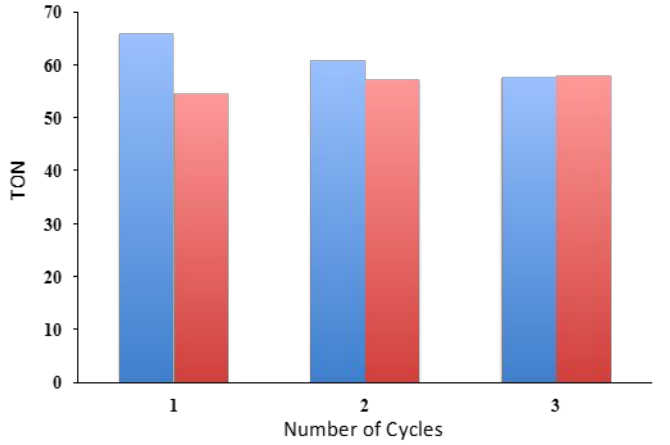

Fig 3. Recyclability of 0.5 (blue) and 1.0 (red) mol % Ru-BBT-POP at 60 °C in the presence KF, Me_2PhSiH, and 1 atm of CO_2.

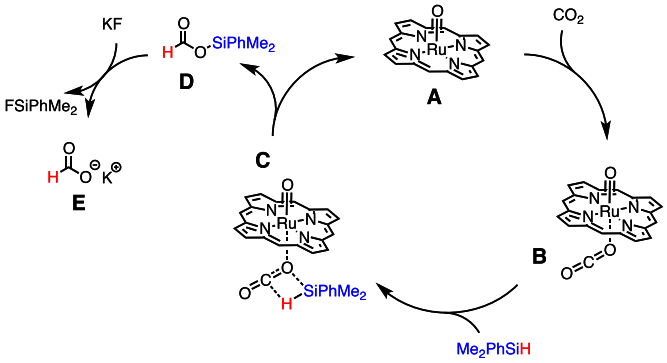

Scheme 2. Proposed mechanism for the hydrosilylative reduction of CO_2 to potassium formate.

With these results in hand, we then evaluated the reactivity of Ru-BBT-POP under the optimal reaction conditions (Entries 3 & 4 Table 1). At a catalyst loading of 0.5 mol %, Ru-BBT-POP afforded a TON of 67 and a TOF of 17 h^{-1} within 4 h at 60 °C at 1 atm of CO_2 (Entry 3 Table 1). Increasing the catalyst loading of Ru-BBT-POP to 1 mol % under the same reaction conditions improved the yield of the reaction but resulted in a slight decrease in the TON (Entry 4 Table 1). The TON values are on par with or higher than other homogeneous Ru-based catalysts that have been reported for the hydrosilylation of CO_2.[27,28] In an effort to examine the recyclability of Ru-BBT-POP after each reaction, the dark red solid was recovered by filtration, washed with MeCN, and used directly in the next reaction. Fig 3 demonstrates that Ru-BBT-POP exhibited a minor reduction in catalytic efficiency at 0.5 mol %, and virtually no reduction in performance at 1 mol % after three cycles (Tables S8 & S9, ESI). FT-IR spectra revealed that the resonance from the carbonyl ligand bound to the Ru(II) center displayed no subtle changes (Fig. S4, ESI), which suggests that the coordination environment around the Ru(II)-porphyrin center remains intact after the reaction. In addition, XPS data taken after catalysis also revealed no apparent changes in the oxidation state of the Ru (Fig. S27, ESI). However, a nitrogen isotherm of Ru-BBT-POP after catalysis revealed a reduction in the surface area and pore volume of the material (Fig. S10 & S11, Table S5, ESI). This reduction could be attributed to the build-up of residual KF inside the pores of Ru-BBT-POP.

Surprisingly, ^1H NMR of the crude reaction mixture prior to addition of KF revealed very little formation of the intermediate dimethylphenylsilyl formate product and a significant amount of a dimethylphenylsilyl ether by-product with a ratio of 1:19, respectively (Fig. S28, ESI). However, the formation of silyl ether by-products during the hydrosilylative reduction of CO_2 is not uncommon and has been observed for Ni-[19] and other Ru-based[29] catalytic systems. This could explain

the low TON and TOF values for this particular system. Based on the experimental data collected, we propose the following mechanism for the hydrosilylative reduction of CO_2 to potassium formate using Ru-BBT-POP (Scheme 2). Initially, CO_2 coordinates to Ru-BBT-POP (A) to generate the activated species (B). Then, CO_2 undergoes σ-bond metathesis with Me_2PhSiH (C) to produce the dimethylphenylsilyl formate (D). From here, the dissociated fluoride ion is able to cleave the dimethylphenyl silyl group to generate the product potassium formate (E).

In summary, a Ru-BBT-POP was constructed and utilized for the hydrosilylative reduction of CO_2 to potassium formate. This work provides a rare example of utilizing a Ru-based POP to perform this chemical transformation. The proof-of-principle is important as POPs metalated with cheap earth-abundant metals (i.e. Cu, Co, Fe, etc.) could be utilized as sustainable catalysts to produce formate/formic acid for energy storage applications. Such investigations are underway in our laboratory and will be reported in the near future.

Acknowledgements

P.L.M. acknowledges the National Science Foundation (NSF) and Georgia Tech Facilitating Academic Careers in Engineering and Science (GT-FACES) for a Career Initiation Grant and funding from the Center for Emergent Materials (DMR-1420451) at The Ohio State University.

Notes and references

1 R. M. DeConto and D. Pollard, *Nature*, 2016, **531**, 591-597.
2 E. E. Benson, C. P. Kubiak, A. J. Sathrum and J. M. Smieja, *Chem. Soc. Rev.* 2009, **38**, 89-99.
3 W. H. Bernskoetter and N. Hazari, *Acc. Chem. Res.* 2017, **50**, 1049-1058.
4 J. Eppinger and K.W. Huang, *ACS Energy Lett.* 2017, **2**, 188-195.
5 C. Federsel, R. Jackstell and M. Beller, *Angew. Chem., Int. Ed.* 2010, *49*, 6254-6257.
6 S. Fukuzimi, Y. Yamada, T. Suenobu, K. Ohkubo and H. Kotani, *Energy Environ. Sci.* 2011, **4**, 2754-2766.
7 J. H. Barnard, C. Wang, N. G. Berry and J. L. Xiang, *Chem. Sci.* 2013, **4**, 1234-1244.
8 Y. Zhang and S. N. Riduan, *Chem. Soc. Rev.* 2012, **41**, 2083-2094.
9 S. Kramer, N. R. Bennedsen and S. Kegnaes, *ACS Catal.* 2018, **8**, 6961-6982.
10 Z. Dai, Q. Sun, X. Liu, C. Bian, Q. Wu, S. Pan, L. Wang, X. Meng, F. Deng and F. S. Xiao*, J. Catal.* 2016, **338**, 202-209.
11 Z. Dai, Q. Sun, X. Liu, L. Guo, J. Li, S. Pan, C. Bian, L. Wang, X. Hu, X. Meng, L. Zhao, F. Deng and F.-S. Xiao, *ChemSusChem* 2017, **10**, 1186-1192.
12 Y. Chen, R. Luo, Q. Xu, W. Zhang, X. Zhou and H. Ji. *ChemCatChem 2017,* **9**, 767-773.
13 W. Wang, Y. Wang, C. Li, L. Yan, M. Jiang and Y. Ding, *ACS Sustainable Chem. Eng.* 2017, **5**, 4523-4528.
14 G. H. Gunasekar, K. Park, V. Ganesan, K. Lee, N.-K. Kim, K.-D. Jung and S. Yoon, *Chem. Mater.* 2017, **29**, 6740-6748.
15 Z.-Z. Yang, H. Zhang, B. Yu, Y. Zhao, G. Ji and Z. Liu, *Chem. Commun.* 2015, **51**, 1271-1274.
16 S. Itagaki, K. Yamaguchi and N. Mizuno, *J. Mol. Catal. A: Chem.* 2013, **366**, 347-352.
17 A. Jensen, H. Görls and S. Pitter, *Organometallics* 2000, **19**, 135-138.
18 S. Park, D. Bézier and M. Brookhart, *J. Am. Chem. Soc.* 2012, **134**, 11404-11407.
19 L. González-Sebastián, M. Flores-Alamo and J. J. García, *Organometallics* 2013, **32**, 7186-7194.
20 T. Matsuo and H. Kawaguchi, *J. Am. Chem. Soc.* 2006, **128**, 12362-12363.
21 K. Motokura, D. Kashiwame, A. Miyaji and T. Baba, *Org. Lett.* 2012, **14**, 2642-2645.
22 G. Feng, C. Du, L. Xiang, I. D. Rosal, G. Li, X. Leng, E. Y.-X. Chen, L. Maron and Y. Chen., *ACS Catal.* 2018, **8**, 4710-4718.
23 M. A. Haga, H.-G. Hong, Y. Shiozawa, Y. Katawa, H. Monjushiro, T. Fukuo and R. Arakawa, *Inorg. Chem.* 2000, **39**, 4566-4573.
24 Y. V. Zubavichus, Y. L. Slovokhotov, M. K. Nazeeruddin, S. M. Zakeeruddin, M. Gratzel and V. Shklover, *Chem. Mater.* 2002, **14**, 3556-3563.
25 D. A. Pyles, J. W. Crowe, L. A. Baldwin, P. L. McGrier, *ACS Macro Lett.* **2016**, *5*, 1055-1058.
26 C. A. Trickett, A. Helal, B. A. Al-Maythalony, Z. H. Yamani, K. E. Cordova, O. M. Yaghi, *Nature Rev. Mater.* **2017**, *2*, 17045.
27 H. Koinuma, F. Kawakami, H. Kato, H. Hirai, *J. Chem. Soc., Chem. Commun.* **1981**, *0*, 213-214.
28 P. G. Jessop, *Top. Catal.* **1998**, *5*, 95-103.
29 T. Juardo-Vázquez, C. Ortiz-Cervantes, J. J. García, *J. Organomet. Chem.* **2016**, *823*, 8-13.

Table of Contents Entry

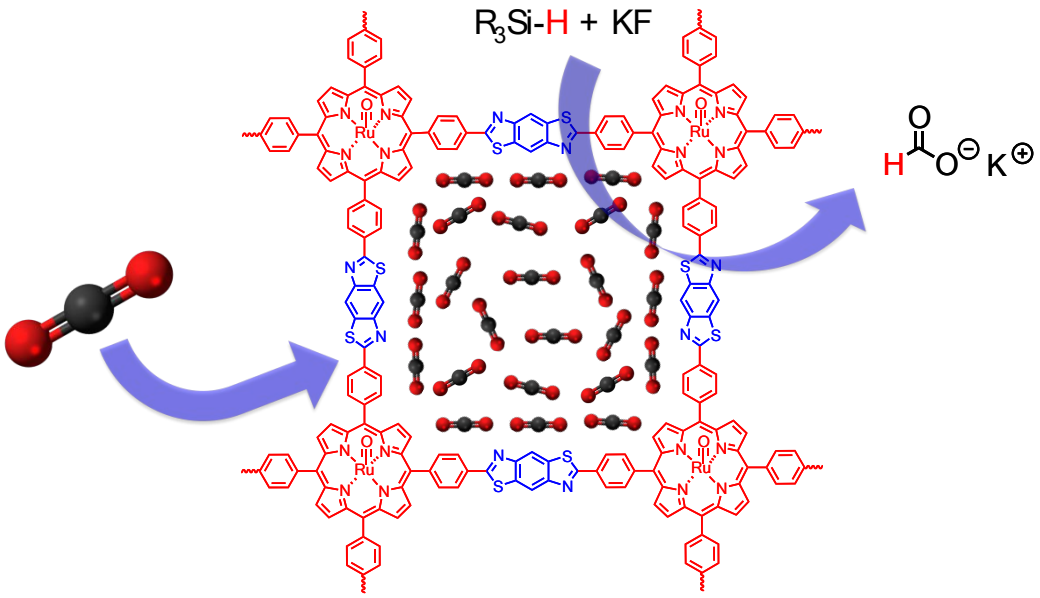

A ruthenium-based porous organic polymer is constructed and used to reduce CO_2 to potassium formate.